ELSEVIER

European Journal of Mechanics B/Fluids 21 (2002) 143–155

EUROPEAN JOURNAL OF MECHANICS B/FLUIDS

On harmonic perturbations in a turbulent mixing layer

Nicolas Reau [a,1], Anatoli Tumin [b,2,*]

[a] *Tel-Aviv University, Tel-Aviv, 69978, Israel*

[b] *The University of Arizona, Tucson, AZ 85721, USA*

Received 23 June 1999; accepted 24 September 2001

Abstract

A theoretical model of harmonic perturbations in a turbulent mixing layer is proposed. The model is based on the triple decomposition method. It is assumed that the instantaneous velocities and pressure consist of three distinctive components: the mean (time average), the coherent (phase average), and the random (turbulent) motion. The interaction between incoherent turbulent fluctuations and large-scale coherent disturbances is incorporated by the Newtonian eddy viscosity model. A slight divergence of the flow is also taken into account, and the results are compared with experimental data. For a high amplitude of the perturbations, the nonlinear feedback to the mean flow is taken into account by means of the coherent Reynolds stresses. The results reveal the possibility of a negative spreading rate of the mixing layer. A simultaneous consideration of the mean flow divergence and nonlinear self-interaction results in Landau-like amplitude equations. It is observed that the nonlinear term in the amplitude equation is not significant at the levels of amplitude considered. The velocity disturbance profiles of the second harmonic are also presented and, at low-level amplitude, they are in good agreement with experiments.

Keywords: Mixing layer; Harmonic perturbations; Stability

1. Introduction

It is common knowledge today that large organized structures may exist in shear turbulent flows and that they are of great importance for mixing processes, sound production from jets, combustion, etc. Studies of the organized motions in turbulent flows have a long history dating from the 1940s. Extensive presentations of earlier works can be found in surveys [1–5].

An appropriate method for analyzing a coherent signal in a turbulent flow is the triple decomposition method. The instantaneous velocities and pressure are considered as sums of three distinctive components: mean (time averaged), coherent (phase averaged), and random (incoherent turbulent) motion. We consider the mean values on the time scales larger than the lifetime of the natural (random) large-scale motion and, therefore, the latter is included into the random component.

The triple decomposition method is a conventional tool in experiments. It serves to describe the coherent disturbances by means of phase-locked measurements. The method has been implicitly used in a number of theoretical works where the stability analysis was applied for turbulent flows. To understand the basic assumptions in these theoretical models, one should consider the governing equations. Reynolds and Hussain [6] derived the equations for a coherent signal in turbulent flow. The equations contain new unknown terms that correspond to oscillations of the background Reynolds stresses caused by the organized wave. These terms reflect the existence of an interaction between the coherent signal and the random field. To a first approximation, the interaction may be neglected and the linearized problem may be reduced to the Rayleigh equation with the mean velocity profile

* Correspondence and reprints.
E-mail address: tumin@engr.arizona.edu (A. Tumin).
[1] Present address: Dassault Aviation, 8, Quai Marcel Dassault, cedex 300, Saint Cloud, 92552 France.
[2] On leave from Tel-Aviv University.

0997-7546/02/$ – see front matter
PII: S0997-7546(01)01170-0

(the effect of molecular viscosity is considered as negligible). Therefore, the results of theoretical models based on the analysis of the Rayleigh equation might be considered as an analysis of coherent structures in a turbulent mixing layer without interaction of the organized and random disturbances. Michalke [7] calculated spatial stability characteristics for the hyperbolic-tangent velocity profile within the scope of the Rayleigh equation. Monkewitz and Huerre [8] performed a comprehensive analysis of spatially growing disturbances using the hyperbolic-tangent and the Blasius shear-layer profiles. Gaster et al. [9] measured the phase and velocity amplitude distributions across a turbulent mixing layer subjected to weak periodic forcing. They also conducted a theoretical analysis within the scope of the linear stability theory. The theoretical results for velocity and phase distributions were in good agreement with the experimental data.

As the free shear flows (such as jets, wakes, and mixing layers) spread rapidly, it is necessary to take into account the flow divergence for a correct comparison of theoretical and experimental data for growth rates and overall amplifications. The main ideas associated with nonparallel effects in shear flows were formulated for boundary layers by Bouthier [10,11] and Gaster [12]. Later Crighton and Gaster [13] and Plaschko [14] applied the method to jets. Gaster et al. [9] also took into consideration the flow divergence in attempting to predict the overall growth of coherent disturbances in the turbulent mixing layer. Nevertheless, the theory overpredicted the overall amplification by two to threefold. The authors suggested that the discrepancy is associated with an interaction of the coherent signal with the random field. (Huerre and Rossi [15] attribute the discrepancy to nonlinear effects.)

It was recognized in the experiments that spreading of the mixing layer flow (and turbulent wakes, as well) is sensitive to coherent perturbations. This means that the problem of a coherent signal in the turbulent flow is coupled with the problem of the mean velocity profile. Ko et al. [16] proposed a theoretical model for the interaction of a coherent signal with the mean flow in a laminar wake. They used an integral method with a nonparallel flow, and the distribution of the fluctuations across the wake was obtained by solving the Rayleigh equation. The fluctuation amplitude and the shape parameters for the mean flow were obtained by solving a set of ordinary differential equations. Cohen et al. [17] also tried to take into consideration the feedback from harmonic perturbations to the mean flow of the mixing layer and to resolve the discrepancy between theoretical and experimental data [9]. The theoretical model was based on a so-called quasi-parallel approach. The Reynolds stress of the coherent signal was calculated using a solution of the Rayleigh equation, and the disturbance amplitude was calculated in accordance with the growth rate obtained from the Rayleigh equation. Since the self-similar velocity profile was obtained as an approximation to the experimental data [9], it was necessary to find only the mixing layer thickness as a function of the downstream coordinate. The equation for the mixing layer scale follows from the integral momentum equation, where the spreading rate is governed by the coherent Reynolds stresses. The results [17] showed agreement between the theoretical and experimental data. However, one should keep in mind that the quasi-parallel approach suffers from an ambiguity of the linear solution normalization. The solution of the Rayleigh equation depends on the downstream coordinate as a parameter, and an undetermined complex function of the downstream coordinate appears. It must be defined in some way or another. The normalization of the eigenfunction influences the resulting level of the Reynolds stresses, as well as the final comparison of the theory with the experimental data. The normalization adopted in the aforementioned paper [17] was not stated. According to J. Cohen and V. Levinski (private communication), the value of the disturbance streamfunction at the centerline was used to normalize the eigenfunctions of the linear problem. In spite of the agreement of the theoretical [17] and experimental data [9], we conclude that the discrepancy between theory and the experiment remains unsolved. We shall consider the problem in Section 3.

Since turbulent shear flows are sensitive to artificial disturbances, the latter may be used for flow control. Oster and Wygnanski [18] investigated the effect of two-dimensional periodic disturbances on the development of a turbulent mixing layer. It was found that the spreading rate of the mixing layer is sensitive to the disturbance frequency and amplitude. Weisbrot and Wygnanski [19] carried out experiments with high-level coherent disturbances in a turbulent mixing layer. They revealed a few regions where the mixing layer developed. In the first region, the spreading rate of the mixing layer increases in the presence of the coherent perturbations. In the second region, the width of the mixing layer, in fact, decreases, and, in the third region, the spreading rate of the mixing layer becomes positive again. In this development process, the coherent Reynolds stresses change their shape significantly: from a positive function across the layer in the first region to a negative function in the second region. A theoretical model of the phenomena is still in question.

As the spreading of the mixing layer is associated with nonlinear effects, a theoretical model must include both nonparallel and nonlinear effects. Huerre and Crighton [20] introduced a heuristic approach combining the slow divergence of the flow and nonlinear effects. Monkewitz [21] incorporated the latter model into an analysis of subharmonic resonances in a mixing layer. More recently, Plaschko [22] proposed a self-consistent approach for considering the nonlinear effects in a mixing layer together with its slow divergence. The solvability condition in the third order provided an amplitude equation containing both effects.

The purpose of the present work is to develop a theoretical model that will resolve the existing discrepancy between theory and experimental data [9], to propose a model of interaction between the coherent disturbance and the mean flow in turbulent mixing layers, and to study nonlinear effects of higher orders.

Briefly, the structure of the paper is as follows. The governing equations are formulated in Section 2. The linear theory in a quasi-parallel and slowly diverging flow is presented in Section 3. In Section 4, a heuristic model for simultaneous consideration of slow divergence and nonlinear effects is proposed based on a linear analysis of the coherent signal with a feedback to the mean flow by means of the coherent Reynolds stresses. A model including nonlinear effects up to the third order and a slow divergence of the mean flow is presented in Section 5. The numerical methods are described in the Appendix.

2. Governing equations

We consider a two-dimensional (in time-average) turbulent flow disturbed by a harmonic two-dimensional wave. We apply the triple decomposition method [6] to analyze the dynamics of the organized wave. It is assumed that the instantaneous velocities and pressure consist of the three distinct components:

$$\begin{aligned} u(x,y,z,t) &= U(x,y) + \tilde{u}(x,y,t) + u'(x,y,z,t),\\ v(x,y,z,t) &= V(x,y) + \tilde{v}(x,y,t) + v'(x,y,z,t),\\ p(x,y,z,t) &= P(x,y) + \tilde{p}(x,y,t) + p'(x,y,z,t), \end{aligned} \tag{1}$$

where U, V, and P are the mean (time-averaged) values of the velocities and pressure correspondingly; $\tilde{u}$, $\tilde{v}$, and $\tilde{p}$ are the coherent (phase-averaged) contributions corresponding to the organized wave; u', v', and p' stand for the random (turbulent motion). We omit the transversal velocity component w in (1), as it consists of the random part only and it will not appear in the governing equations because of the assumption about the two-dimensional mean flow. After substituting (1) into Navier–Stokes equations and, phase and time averaging, the equations for the mean flow and for the organized wave can be obtained [6]. We assume that the effects of molecular viscosity are negligible and omit the corresponding terms:

$$\begin{aligned} &\frac{\partial U}{\partial x} + \frac{\partial V}{\partial y} = 0,\\ &U\frac{\partial U}{\partial x} + V\frac{\partial U}{\partial y} = -\frac{1}{\rho}\frac{\partial P}{\partial x} - \frac{\partial \overline{u'v'}}{\partial y} - \frac{\partial \overline{u'^2}}{\partial x} - \frac{\partial \overline{\tilde{u}\tilde{v}}}{\partial y} - \frac{\partial \overline{\tilde{u}^2}}{\partial x},\\ &U\frac{\partial V}{\partial x} + V\frac{\partial V}{\partial y} = -\frac{1}{\rho}\frac{\partial P}{\partial x} - \frac{\partial \overline{u'v'}}{\partial x} - \frac{\partial \overline{v'^2}}{\partial x} - \frac{\partial \overline{\tilde{u}\tilde{v}}}{\partial x} - \frac{\partial \overline{\tilde{v}^2}}{\partial y}. \end{aligned} \tag{2}$$

The last couples of terms in the x- and y-momentum equations make the equations different from the usual mean equations for turbulent flow and provide the feedback from the organized wave to the mean flow. The dynamical equations for the organized wave are

$$\begin{aligned} &\frac{\partial \tilde{u}}{\partial x} + \frac{\partial \tilde{v}}{\partial y} = 0,\\ &\frac{\partial \tilde{u}}{\partial t} + U\frac{\partial \tilde{u}}{\partial x} + V\frac{\partial \tilde{u}}{\partial y} + \tilde{u}\frac{\partial U}{\partial x} + \tilde{v}\frac{\partial U}{\partial x}\\ &\quad = -\frac{1}{\rho}\frac{\partial \tilde{p}}{\partial x} + \frac{\partial}{\partial x}\left(\overline{\tilde{u}^2} - \tilde{u}^2\right) + \frac{\partial}{\partial y}\left(\overline{\tilde{u}\tilde{v}} - \tilde{u}\tilde{v}\right) - \frac{\partial}{\partial x}\left(\langle u'^2\rangle - \overline{u'^2}\right) - \frac{\partial}{\partial y}\left(\langle u'v'\rangle - \overline{u'v'}\right),\\ &\frac{\partial \tilde{v}}{\partial t} + U\frac{\partial \tilde{v}}{\partial x} + V\frac{\partial \tilde{v}}{\partial y} + \tilde{u}\frac{\partial V}{\partial x} + \tilde{v}\frac{\partial V}{\partial x}\\ &\quad = -\frac{1}{\rho}\frac{\partial \tilde{p}}{\partial y} + \frac{\partial}{\partial x}\left(\overline{\tilde{u}\tilde{v}} - \tilde{u}\tilde{v}\right) + \frac{\partial}{\partial y}\left(\overline{\tilde{v}^2} - \tilde{v}^2\right) - \frac{\partial}{\partial x}\left(\langle u'v'\rangle - \overline{u'v'}\right) - \frac{\partial}{\partial y}\left(\langle v'^2\rangle - \overline{v'^2}\right), \end{aligned} \tag{3}$$

where the over-bar and brackets represent mean and phase averaging, respectively.

Eqs. (2) and (3) are not closed, and we need to choose a closure hypothesis. The boundary-layer approximation is assumed for the mean flow equations (2), and we invoke closure by means of the eddy viscosity,

$$\overline{u'v'} = -\nu_t(x)\frac{\partial U}{\partial y}, \tag{4}$$

where $\nu_t(x)$ is a linear function of x. The eddy viscosity model (4) is applied to the incoherent part of the flow, and the problem is to analyze a coherent signal imposed on the turbulent flow.

We recast the mean flow equations as follows:

$$\begin{aligned} &\frac{\partial U}{\partial x}+\frac{\partial V}{\partial y}=0,\\ &U\frac{\partial U}{\partial x}+V\frac{\partial U}{\partial y}=-\frac{\partial\overline{\tilde{u}\tilde{v}}}{\partial y}-\frac{\partial\overline{\tilde{u}^2}}{\partial x}+\nu_t(x)\frac{\partial^2 U}{\partial y^2}. \end{aligned} \tag{5}$$

Eq. (5) contains coherent Reynolds stresses and, therefore, there is a possibility for the feedback from the coherent signal to the mean flow. To solve (5), one needs to define a velocity profile $U(x_0, y)$ at $x = x_0$ and boundary conditions at $y \to \pm\infty$:

$$y\to+\infty:\quad U\to U_1;\qquad y\to-\infty:\quad U\to U_2. \tag{6}$$

For further considerations, we shall use U_1 as the velocity scale. We also introduce the scale of the mixing layer $\delta(x)$ by means of

$$\frac{\delta(x)U_1}{\nu_t(x)}\frac{\mathrm{d}\delta}{\mathrm{d}x}=\frac{1}{2}. \tag{7}$$

We are looking for the velocity profile $U(x, y)$ in the form

$$U(x,y)=U_1 f'(x,\eta), \tag{8}$$

where the prime stands for the derivative with respect to $\eta = y/\delta(x)$, and the coordinate $\eta = 0$ corresponds to the point where $f = 0$ (actually, it is the third boundary conditions imposed on the mean flow solution). Substituting (8) into (5) and taking into account (7), we obtain the following equation and the boundary conditions for the mean flow

$$f'''+\frac{1}{2}ff''=\frac{x}{2}\left(f'\frac{\partial f'}{\partial x}-f''\frac{\partial f}{\partial x}\right)+\Phi(x,\eta), \tag{9}$$

$$\eta\to+\infty:\quad f'\to 1;\qquad \eta\to-\infty:\quad f'\to r=U_2/U_1. \tag{10}$$

The last term, Φ, in (9) contains the coherent Reynolds stresses. If the coherent disturbances are negligible, (9) is the well-known boundary-layer equation for a turbulent mixing layer and, at some distance from the starting point x_0, the solution converges to the self-similar solution of the Blasius equation (the right side of (9) is equal to zero).

As follows from experiments, $\mathrm{d}\delta/\mathrm{d}x$ is a linear function of the velocity ratio parameter $R = (U_1 - U_2)/(U_1 + U_2)$. Usually the momentum thickness $\theta(x)$,

$$\theta(x)=\int_{-\infty}^{+\infty}\frac{U-U_2}{U_1-U_2}\left(1-\frac{U-U_2}{U_1-U_2}\right)\mathrm{d}y, \tag{11}$$

is used as a length scale, and one can find experimental data for the spreading rate in [5]. We approximate the experimental data as

$$\frac{\mathrm{d}\theta}{\mathrm{d}x}=0.046R. \tag{12}$$

Thus, for a prescribed velocity ratio R, we can solve the equations for the undisturbed mixing layer and obtain δ/θ. Then, we can find $\mathrm{d}\delta/\mathrm{d}x$ from (12) and calculate the turbulent Reynolds number $Re_t = U_1\delta/\nu_t$ from (7). Fig. 1 shows $Re_\theta = |U_1 - U_2|\theta/\nu_t$ as a function of R. We would like to point out that the approximation of experimental data (12) and the results presented in Fig. 1 are universal for undisturbed turbulent mixing layers. The figure provides the correspondence of the velocity ratio parameter to the turbulent Reynolds number. One can see that the typical Reynolds numbers, Re_θ, are about 15. The results will be utilized in further analyses of coherent perturbations in turbulent mixing layers.

The equations for organized waves (3) contain new terms,

$$\tilde{r}_{ij}=\langle u_i'u_j'\rangle-\overline{u_i'u_j'}, \tag{13}$$

corresponding to oscillation of the background Reynolds stress caused by the organized wave [6]. The term is responsible for the interaction of a coherent signal with the random field, and we need to choose a hypothesis to close the equations. Accordingly to [6], we adopt the Newtonian eddy viscosity model

$$\tilde{r}_{ij}=-\nu_t\left(\frac{\partial\tilde{u}_i}{\partial x_j}+\frac{\partial\tilde{u}_j}{\partial x_i}\right), \tag{14}$$

where $\nu_t(x)$ is the eddy viscosity of the undisturbed flow. Making use of (14), we obtain a set of equations for a coherent signal from (3),

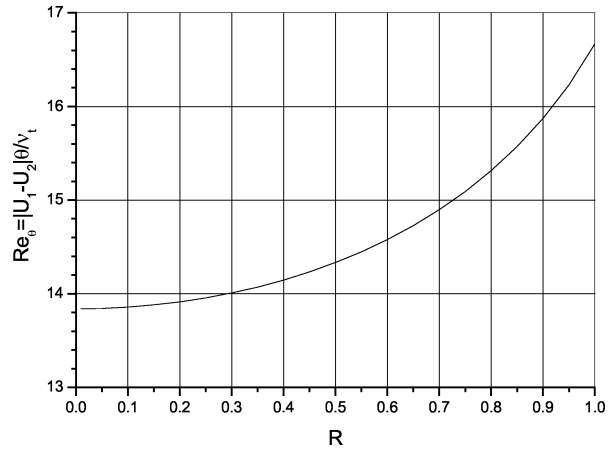

Fig. 1. Reynolds number vs velocity ratio parameter.

$$\frac{\partial \tilde{u}}{\partial x}+\frac{\partial \tilde{v}}{\partial y}=0,$$
$$\frac{\partial \tilde{u}}{\partial t}+U\frac{\partial \tilde{u}}{\partial x}+V\frac{\partial \tilde{u}}{\partial y}+\tilde{u}\frac{\partial U}{\partial x}+\tilde{v}\frac{\partial U}{\partial x}=-\frac{1}{\rho}\frac{\partial \tilde{p}}{\partial x}+\frac{\partial}{\partial x}\left(\overline{\tilde{u}^2}-\tilde{u}^2\right)+\frac{\partial}{\partial y}\left(\overline{\tilde{u}\tilde{v}}-\tilde{u}\tilde{v}\right)+\nu_t\left(\frac{\partial^2\tilde{u}}{\partial x^2}+\frac{\partial^2\tilde{u}}{\partial y^2}\right), \tag{15}$$
$$\frac{\partial \tilde{v}}{\partial t}+U\frac{\partial \tilde{v}}{\partial x}+V\frac{\partial \tilde{v}}{\partial y}+\tilde{u}\frac{\partial V}{\partial x}+\tilde{v}\frac{\partial V}{\partial x}=-\frac{1}{\rho}\frac{\partial \tilde{p}}{\partial y}+\frac{\partial}{\partial x}\left(\overline{\tilde{u}\tilde{v}}-\tilde{u}\tilde{v}\right)+\frac{\partial}{\partial y}\left(\overline{\tilde{v}^2}-\tilde{v}^2\right)+\nu_t\left(\frac{\partial^2\tilde{v}}{\partial x^2}+\frac{\partial^2\tilde{v}}{\partial y^2}\right),$$

where we omitted the term $\mathrm{d}\nu_t/\mathrm{d}x$, that is the term of higher order. Equation (15) should be completed by the boundary conditions

$$y\to\pm\infty:\quad \tilde{u},\tilde{v},\tilde{p}\to 0. \tag{16}$$

3. Linear theory – slowly diverging flow

As observed in experiments, a coherent signal may influence the spreading rate of the mixing layer, and the traditional consideration of non-parallel effects is in conflict with the essence of the phenomenon that stems from nonlinear interactions of large-scale disturbances. At this stage, consider the conventional approach and, after the analysis of nonlinear effects, we will conclude (see Section 5) that the approach is acceptable at the amplitude of interest.

In what follows, we use the length scale $\delta(x)$ and omit the 'tilde' above the coherent components. We introduce the vector-function

$$\mathbf{A}=\begin{vmatrix} u \\ p \\ v \\ \frac{\partial u}{\partial y}-\frac{\partial v}{\partial x} \end{vmatrix}, \tag{17}$$

and rewrite the linearized equations as

$$\frac{\partial \mathbf{A}}{\partial y}+H_{10}\frac{\partial \mathbf{A}}{\partial t}=H_{11}\mathbf{A}+H_2\frac{\partial \mathbf{A}}{\partial x}+\mu H_3\mathbf{A}, \tag{18}$$

where H_{10}, H_{11}, H_2, and H_3 are 4×4 matrices and the matrix H_3 is associated with the terms originated from a slow diverging of the mean flow,

$$H_{10}=\begin{pmatrix} 0 & 0 & 0 & 0 \\ 0 & 0 & 1 & 0 \\ 0 & 0 & 0 & 0 \\ -Re_t & 0 & 0 & 0 \end{pmatrix}, \qquad H_{11}=\begin{pmatrix} 0 & 0 & 0 & 1 \\ 0 & 0 & 0 & 0 \\ 0 & 0 & 0 & 0 \\ 0 & 0 & U'Re_t & 0 \end{pmatrix},$$

$$H_2 = \begin{pmatrix} 0 & 0 & 1 & 0 \\ 0 & 0 & -U & -Re_t^{-1} \\ -1 & 0 & 0 & 0 \\ Re_t U & Re_t & 0 & 0 \end{pmatrix}, \qquad H_3 = \begin{pmatrix} 0 & 0 & 0 & 0 \\ V_0 \frac{\partial}{\partial X} + \mathrm{O}(\mu) & 0 & -\frac{\partial V_0}{\partial y} & 0 \\ 0 & 0 & 0 & 0 \\ \frac{\partial U}{\partial X} Re_t & 0 & Re_t V_0 \frac{\partial}{\partial X} & Re_t V_0 \end{pmatrix}, \tag{19}$$

where a 'slow' variable, $X = \mu x$, appears in H_3, and $V_0(X, y) = \mu^{-1} V$, $U = U(X, y)$.

We are looking for a solution in the form

$$\mathbf{A}(x, X, y, t) = \exp\left[i \int_{x_0}^{x} \alpha \, \mathrm{d}x - i\omega t \right] \left[a(X)\mathbf{A}_1(X, y) + \mu \mathbf{A}_1(X, y) + \cdots \right]. \tag{20}$$

To leading orders of μ, we obtain the conventional system of the linear stability theory,

$$\frac{\partial \mathbf{A}_1}{\partial y} = H_1 \mathbf{A}_1 + i\alpha H_2 \mathbf{A}_1, \tag{21}$$

where $H_1 = H_{11} + i\omega H_{10}$. We should complete the equations with the boundary conditions of the decaying solution at $y \to \pm\infty$. The system (21) may be reduced to the Orr–Sommerfeld equation for the third component of the vector $\mathbf{A}_1$. The coefficients in (21) are slow functions of the variable X, and the problem of consistent normalization for the quasi-parallel solution $\mathbf{A}_1$ arises. The ambiguity is resolved through consideration of the next-order equations.

In the next order, we have an inhomogeneous system

$$\frac{\partial \mathbf{A}_2}{\partial y} - H_1 \mathbf{A}_2 - i\alpha H_2 \mathbf{A}_2 = \frac{\partial a}{\partial X} H_2 \mathbf{A}_1 + a H_2 \frac{\partial \mathbf{A}_1}{\partial X} + a H_3 \mathbf{A}_1. \tag{22}$$

The solvability condition of the system (22) will be the orthogonality of the right side to solution $\mathbf{B}$ of the adjoint problem,

$$-\frac{\partial \mathbf{B}}{\partial y} = H_1^* \mathbf{B} - i\bar{\alpha} H_2^* \mathbf{B}, \tag{23}$$

with the boundary conditions of the decaying solution at $y \to \pm\infty$. The asterisk (*) in (23) stands for the Hermitian adjoint matrix, and the over-bar stands for the complex conjugate. We rewrite the solvability condition for (22) in the following form:

$$\frac{\partial a}{\partial X} \langle H_2 \mathbf{A}_1, \mathbf{B} \rangle + a(X) \left[\left\langle H_2 \frac{\partial \mathbf{A}_1}{\partial X}, \mathbf{B} \right\rangle + \langle H_3 \mathbf{A}_1, \mathbf{B} \rangle \right] = 0, \tag{24}$$

where the inner product $\langle \, , \, \rangle$ is defined as

$$\langle \mathbf{A}, \mathbf{B} \rangle = \sum_{j=1}^{4} \int_{-\infty}^{+\infty} A_j \bar{B}_j \, \mathrm{d}y. \tag{25}$$

The solvability condition (24) is an equation for the slow function $a(X)$, resulting in a uniquely determined normalization of the linear problem solution. One can show that the coefficients

$$M(X) = \langle H_2 \mathbf{A}_1, \mathbf{B} \rangle, \qquad N(X) = \left\langle H_2 \frac{\partial \mathbf{A}_1}{\partial X}, \mathbf{B} \right\rangle + \langle H_3 \mathbf{A}_1, \mathbf{B} \rangle \tag{26}$$

are equal to the coefficients derived in [12] for boundary-layer flows. By neglecting the viscous-related terms, one can obtain from (26) the coefficients given in [9].

Because one of the goals of the present work is to resolve the discrepancy between the theory and experiment [9], we consider the turbulent mixing layer having the velocity-ratio parameters $R = 0.25$ and $R = 0.43$, corresponding to set I and to set III in the experiments. As the amplitudes were relatively small, one can neglect the feedback to the mean flow and to use the Blasius velocity profile with Re_θ from Fig. 1. Another option is to use the experimental velocity profile from [9] and to evaluate the corresponding value of Re_θ in accordance with the measured spreading rate. Our comparisons of these velocity profiles have shown that they are very close. The corresponding Reynolds numbers are presented in Table 1.

The results for both finite and infinite Reynolds numbers are given in Fig. 2. One can see that the interaction of the coherent signal with the random field emulated by the eddy viscosity provides good agreement between the theory and experimental data. In the course of the present work, we used conventional numerical methods for solving the mean flow and stability equations (see Appendix).

Table 1
Reynolds numbers used in the calculations

	Set I	Set III
Blasius mixing layer	13.4	14.5
Experimental velocity profile	11.6	12.6

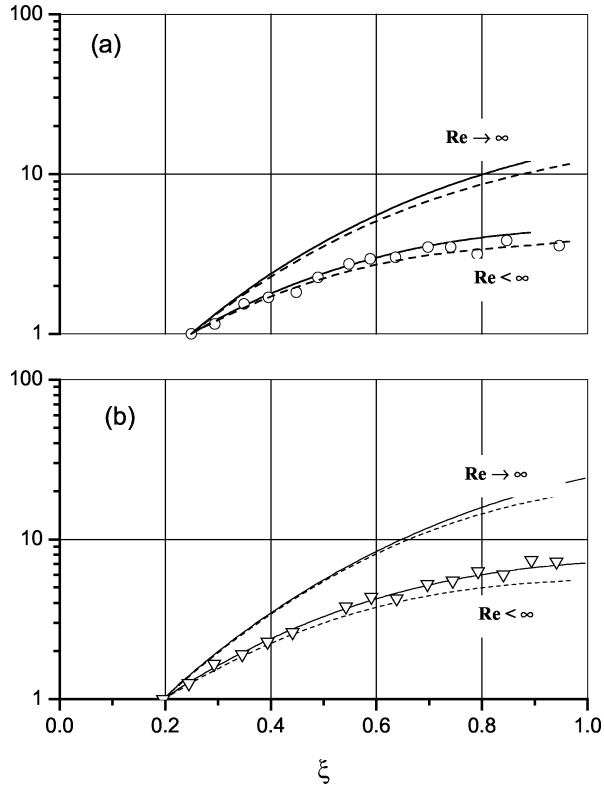

Fig. 2. The overall amplification $\int_{-\infty}^{+\infty} |u| \, dy$ of disturbances with respect to dimensionless downstream coordinate [12]: (a) set I; (b) set III. Solid lines = the Blasius mixing layer; dash lines – approximated velocity profiles. Symbols = experimental data.

4. A heuristic model of interaction between the mean flow and a coherent signal

We continue with the consideration of the feedback from the coherent signal to the mean flow. As was shown in experiments [18,19], the spreading rate of a mixing layer depends on the amplitude of the harmonic perturbations. Thus, we would like to keep the coherent Reynolds stresses, as well as the eddy viscosity term, in the equations of the mean flow (5). Instead of an asymptotic correction of the mean flow in the second order of the amplitude, we will solve the original equations (5) numerically, where the coherent Reynolds stresses are evaluated from the linear problem considered in Section 3.

For the numerical consideration of the interaction between coherent disturbances and a mean flow, we will consider parameters from set I of the experimental data [9], with $U_1 = 5$ m/s, $U_1 = 3$ m/s, and $f = 20$ Hz. The experiment by Weisbrot and Wygnanki [19] was carried out at $U_1 = 10$ m/s, $U_1 = 6$ m/s, and $f = 44.5$ Hz. Since the velocities in [19] were higher by a factor of 2 than those in set I of [9], and the frequency differs approximately by the same factor, we can also compare our theoretical results with the experimental data of [19].

We start calculations with a velocity profile as the step function:

$$y > 0: \quad U = U_1; \qquad y < 0: \quad U = U_2. \tag{27}$$

At $x = 0.1$ m, the velocity profile is already close to the self-similar Blasius solution, and we smoothly introduce the disturbance at the interval $x = 0.1055{-}0.125$ m. The smoothing factor $\sin(\pi(x - x_0)/0.41)$ appears at the term Φ in (9). The amplitude equation (24) and the mean velocity equation (9), where Reynolds stresses are calculated with the fundamental harmonic, are solved simultaneously. We use as the initial amplitude of the coherent signal the amplitude of the normal velocity component

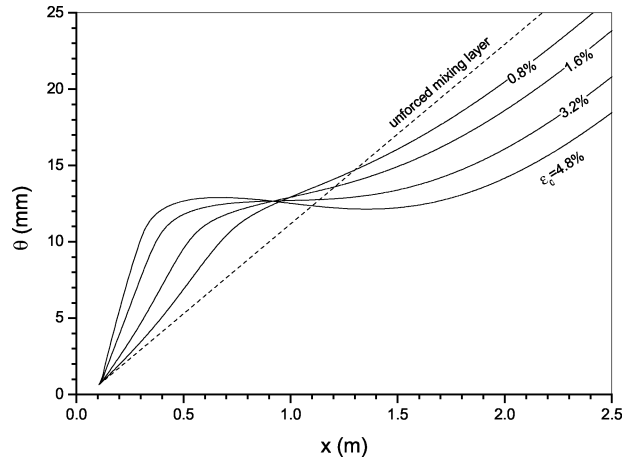

Fig. 3. Momentum thickness for the mixing layer in the presence of a coherent signal.

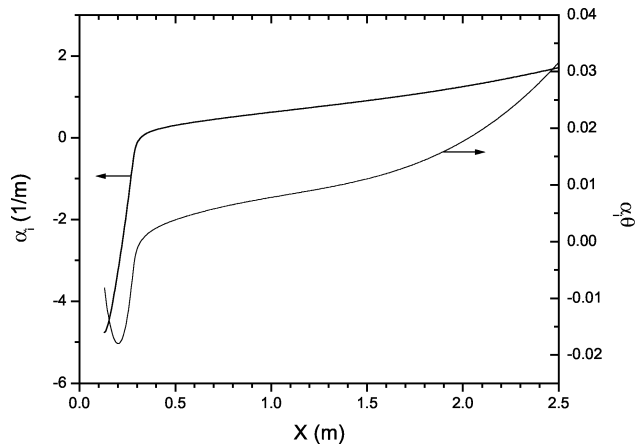

Fig. 4. Imaginary part of the eigenvalue at $\varepsilon_0 = 4.8\%$.

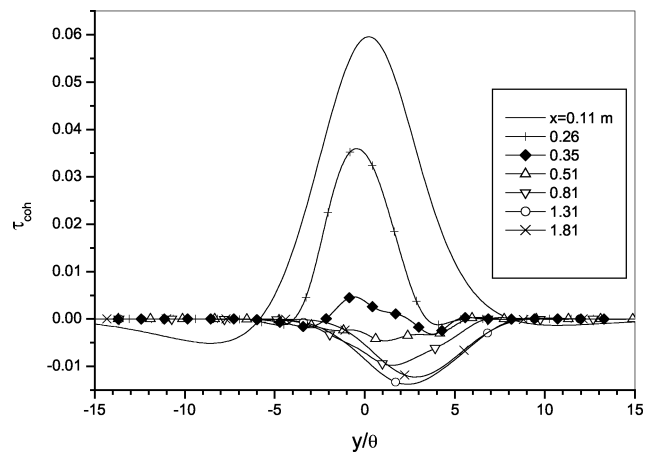

Fig. 5. Coherent Reynolds stresses $\tau_{\text{coh}} = -\overline{uv}$ at $\varepsilon_0 = 4.8\%$.

$\varepsilon_0 = v/U_1$ at $y = 0$, at the starting point $x_0 = 0.1055$ m. Results for the momentum thickness θ as a function of the downstream coordinate x are shown in Fig. 3.

One can see that at $\varepsilon_0 = 4.8\%$ there is an interval with a negative derivative $\mathrm{d}\theta/\mathrm{d}x$. The interval with the negative spreading rate was observed in the experiments at $x = 0.56-0.84$ m, while it appears up to $x = 1.4$ m in our study.

The imaginary part of the eigenvalue α_1 is shown in Fig. 4. The disturbance becomes stable at $x \approx 0.4$ m, and the coherent Reynolds stress $-\overline{uv}$ changes its sign in the stable zone (see Fig. 5). One can see that, in the unstable zone, the Reynolds stress is mainly positive, and, farther downstream, the coherent Reynolds stress is negative, as was observed in the experiments. As the Reynolds stress is negative, it acts as a driving force in Eq. (9) and causes flow acceleration.

5. A nonlinear model for the coherent signal in a slowly diverging flow

For small amplitudes of the disturbance, the spreading rate will be governed mainly by the incoherent large-scale eddies. When the amplitude of the coherent disturbance is high, the spreading rate will be proportional to ε^2, where ε is an amplitude parameter. Thus, we assume that the spreading rate parameter μ may be of the same order of magnitude as ε^2.

We introduce the 'slow' variable $X = \varepsilon^2 x$ as suggested in [22], and represent the coherent disturbance of velocity and pressure as the series

$$\begin{aligned} u(x, X, y, t) &= \varepsilon u_1(x, X, y, t) + \varepsilon^2 u_2(x, X, y, t) + \varepsilon^3 u_3(x, X, y, t) + \cdots, \\ v(x, X, y, t) &= \varepsilon v_1(x, X, y, t) + \varepsilon^2 v_2(x, X, y, t) + \varepsilon^3 v_3(x, X, y, t) + \cdots, \\ p(x, X, y, t) &= \varepsilon p_1(x, X, y, t) + \varepsilon^2 p_2(x, X, y, t) + \varepsilon^3 p_3(x, X, y, t) + \cdots. \end{aligned} \tag{28}$$

The mean velocity profiles $U(X, y)$ and $V(X, y) = \varepsilon^2 V_0(X, y)$ are solutions of Eqs. (5), and we do not use for them an expansion series. By substituting (29) into (16) and collecting the terms of the same order of magnitude, we obtain the governing equations for the coherent disturbance. In the leading term, we obtain equations for the fundamental disturbance:

$$\begin{aligned} &\frac{\partial u_1}{\partial x} + \frac{\partial v_1}{\partial y} = 0, \\ &\frac{\partial u_1}{\partial t} + U\frac{\partial u_1}{\partial x} + v_1\frac{\partial U}{\partial y} = -\frac{\partial p_1}{\partial x} + \frac{1}{Re_t}\left(\frac{\partial^2 u_1}{\partial x^2} + \frac{\partial^2 u_1}{\partial y^2}\right), \\ &\frac{\partial v_1}{\partial t} + U\frac{\partial v_1}{\partial x} = -\frac{\partial p_1}{\partial y} + \frac{1}{Re_t}\left(\frac{\partial^2 v_1}{\partial x^2} + \frac{\partial^2 v_1}{\partial y^2}\right). \end{aligned} \tag{29}$$

We present the fundamental perturbations of frequency ω as

$$\begin{aligned} u_1(x, X, y, t) &= 0.5\big[a(X)u_1^{(0)}(X, y)\mathrm{e}^{i\varphi(x)t - i\omega t} + \text{c.c.}\big], \\ v_1(x, X, y, t) &= 0.5\big[a(X)v_1^{(0)}(X, y)\mathrm{e}^{i\varphi(x)t - i\omega t} + \text{c.c.}\big], \\ p_1(x, X, y, t) &= 0.5\big[a(X)p_1^{(0)}(X, y)\mathrm{e}^{i\varphi(x)t - i\omega t} + \text{c.c.}\big], \end{aligned} \tag{30}$$

where c.c. stands for complex conjugate, and the phase $\varphi$is related to the complex slow function $\alpha_1(X)$ as

$$\frac{\mathrm{d}\varphi}{\mathrm{d}x} = \alpha_1(X). \tag{31}$$

It is assumed that the derivative of the slow amplitude function may be written in the following form:

$$\frac{\mathrm{d}a}{\mathrm{d}X} = F_0^{(1)}(X) + \varepsilon F_1^{(1)}(X) + \varepsilon^2 F_2^{(1)}(X) + \cdots. \tag{32}$$

The unknown functions $F_0^{(1)}(X)$, $F_1^{(1)}(X), \ldots$, may be found from the solvability conditions for equations of the higher orders of ε.

Substitution of (31) into (29) yields

$$\begin{aligned} &i\alpha_1 u_1^{(0)} + \frac{\partial v_1^{(0)}}{\partial y} = 0, \\ &i(\alpha_1 U - \omega)u_1^{(0)} + v_1^{(0)}\frac{\partial U}{\partial y} = -i\alpha_1 p_1^{(0)} + \frac{1}{Re_t}\left(\frac{\partial^2 u_1^{(0)}}{\partial y^2} - \alpha_1^2 u_1^{(0)}\right), \end{aligned}$$

$$i(\alpha_1 U-\omega)v_1^{(0)} = -\frac{\partial p_1^{(0)}}{\partial y} + \frac{1}{Re_t}\left(\frac{\partial^2 v_1^{(0)}}{\partial y^2} - \alpha_1^2 v_1^{(0)}\right). \tag{33}$$

We also introduce a function z_4:

$$z_4(x,X,y,t) = \frac{\partial u}{\partial y} - \frac{\partial v}{\partial x} = \varepsilon z_{41}(x,X,y,t) + \varepsilon^2 z_{42}(x,X,y,t) + \varepsilon^3 z_{43}(x,X,y,t) + \cdots, \tag{34}$$

and write the first term as

$$z_{41}(x,X,y,t) = 0.5\big[a(X)z_{41}^{(0)}(X,y)\mathrm{e}^{i\varphi(x)-i\omega t} + \text{c.c.}\big]. \tag{35}$$

If we introduce the vector-function

$$A_1 = \begin{vmatrix} u_1^{(0)} \\ p_1^{(0)} \\ v_1^{(0)} \\ z_{41}^{(0)} \end{vmatrix}, \tag{36}$$

we obtain the equations in the main order of magnitude, which is the same as Eq. (21),

$$\frac{\partial \mathbf{A}_1}{\partial y} = H_1(\omega)\mathbf{A}_1 + i\alpha_1 H_2 \mathbf{A}_1. \tag{37}$$

In the second order, we have the inhomogeneous equations for the second harmonic. Velocities and pressure are presented in the following form:

$$\begin{aligned} u_2 &= 0.25\big[a^2 u_2^{(0)}(X,y)\mathrm{e}^{2i\varphi(x)t-2i\omega t} + \text{c.c.}\big], \\ v_2 &= 0.25\big[a^2 v_2^{(0)}(X,y)\mathrm{e}^{2i\varphi(x)t-2i\omega t} + \text{c.c.}\big], \\ p_2 &= 0.25\big[a^2 p_2^{(0)}(X,y)\mathrm{e}^{2i\varphi(x)t-2i\omega t} + \text{c.c.}\big]. \end{aligned} \tag{38}$$

If we introduce the vector function

$$\mathbf{A}_2 = \begin{vmatrix} u_2^{(0)} \\ p_2^{(0)} \\ v_2^{(0)} \\ z_{42}^{(0)} \end{vmatrix}, \tag{39}$$

the equations may be written as

$$\frac{\partial \mathbf{A}_2}{\partial y} - H_1(2\omega)\mathbf{A}_2 - 2i\alpha_1 H_2 \mathbf{A}_2 = \mathbf{S}, \tag{40}$$

where the vector $\mathbf{S}$ has the only single non-zero component S_4 (the component S_2 becomes equal to zero due to the continuity equation),

$$S_4 = 2i\,Re_t \alpha_1 u_1^{(0)^2} + Re_t \frac{\partial v_1^{(0)} u_1^{(0)}}{\partial y}. \tag{41}$$

As a result of the nonlinear interaction between the second harmonic and the fundamental harmonic, we obtain the terms with frequencies ω and 3ω. We shall consider only the terms of fundamental frequency ω because they can be used to find the slow function $F_0^{(1)}(X)$ from the solvability condition. The ω-harmonic is presented as

$$\begin{aligned} u_3(x,X,y,t) &= 0.5\big[u_3^{(0)}(X,y)\mathrm{e}^{i\varphi(x)-i\omega t} + \text{c.c.}\big], \\ v_3(x,X,y,t) &= 0.5\big[v_3^{(0)}(X,y)\mathrm{e}^{i\varphi(x)-i\omega t} + \text{c.c.}\big], \\ p_3(x,X,y,t) &= 0.5\big[p_3^{(0)}(X,y)\mathrm{e}^{i\varphi(x)-i\omega t} + \text{c.c.}\big], \\ z_{43}(x,X,y,t) &= 0.5\big[z_{43}^{(0)}(X,y)\mathrm{e}^{i\varphi(x)-i\omega t} + \text{c.c.}\big], \end{aligned} \tag{42}$$

and we introduce the vector-function

$$\mathbf{A}_3 = \begin{vmatrix} u_3^{(0)} \\ p_3^{(0)} \\ v_3^{(0)} \\ z_{43}^{(0)} \end{vmatrix}. \tag{43}$$

The inhomogeneous equations will be written as

$$\frac{\partial \mathbf{A}_3}{\partial y} - H_1(\omega)\mathbf{A}_3 - i\alpha_1 H_2 \mathbf{A}_3 = F_0^{(1)}(X) H_2 \mathbf{A}_1 + a H_2 \frac{\partial \mathbf{A}_1}{\partial X} + a H_3 \mathbf{A}_1 + 0.25 a^2 \bar{a} \mathrm{e}^{-2\mathrm{Im}(\varphi)} \mathbf{Q}, \tag{44}$$

where vector $\mathbf{Q}$ has two non-zero components, Q_2 and Q_4,

$$\begin{aligned} Q_2 &= i\bar{\alpha}_1 u_2^{(0)} \bar{v}_1^{(0)} - 2i\alpha_1 \bar{u}_1^{(0)} v_2^{(0)} - v_2^{(0)} \frac{\partial \bar{v}_1^{(0)}}{\partial y} - \bar{v}_1^{(0)} \frac{\partial v_2^{(0)}}{\partial y}, \\ Q_4 &= 2i\alpha_1 Re_t u_2^{(0)} \bar{u}_1^{(0)} - i\bar{\alpha}_1 Re_t u_1^{(0)} \bar{u}_2^{(0)} + Re_t \bar{v}_1^{(0)} \frac{\partial u_2^{(0)}}{\partial y} + Re_t v_2^{(0)} \frac{\partial \bar{u}_1^{(0)}}{\partial y}. \end{aligned} \tag{45}$$

The solvability condition for the system (44) is the orthogonality condition of its right side with respect to the solution $\mathbf{B}$ of the adjoint problem (23)

$$F_0^{(1)}(X)\langle H_2 \mathbf{A}_1, \mathbf{B}\rangle + a(X)\left[\left\langle H_2 \frac{\partial \mathbf{A}_1}{\partial X}, \mathbf{B}\right\rangle + \langle H_3 \mathbf{A}_1, \mathbf{B}\rangle\right] + 0.25 a^2 \bar{a} \mathrm{e}^{-2\mathrm{Im}(\varphi)} \langle \mathbf{Q}, \mathbf{B}\rangle = 0. \tag{46}$$

Since we obtain the unknown function $F_0^{(1)}(X)$ from (46), the expansion (32) yields the equation for the slow amplitude function

$$\frac{\mathrm{d}a}{\mathrm{d}X} = -a \frac{\left[\left\langle H_2 \frac{\partial \mathbf{A}_1}{\partial X}, \mathbf{B}\right\rangle + \langle H_3 \mathbf{A}_1, \mathbf{B}\rangle\right]}{\langle H_2 \mathbf{A}_1, \mathbf{B}\rangle} - 0.25 a^2 \bar{a} \mathrm{e}^{-2\mathrm{Im}(\varphi)} \frac{\langle \mathbf{Q}, \mathbf{B}\rangle}{\langle H_2 \mathbf{A}_1, \mathbf{B}\rangle}. \tag{47}$$

The first term in right side of Eq. (47) represents the conventional input due to the flow divergence, and the second term is associated with the nonlinear self-interaction of the disturbance.

We solve the system of equations (40) with the boundary conditions of the decaying solution at $y \to \pm\infty$. The streamwise velocity disturbance profiles of the fundamental and second harmonics at $\varepsilon_0 = 0.1\%$ (normalized to 1 at the maximum) are shown in Fig. 6. The shape of the second harmonic agrees with the experimental data of [23]. The experimental conditions in [23] were the same as in [9] (except a frequency of 22 Hz was used instead of 20 Hz as used in [9]). Thus, the shapes of the velocity distributions may be compared qualitatively at the same streamwise locations.

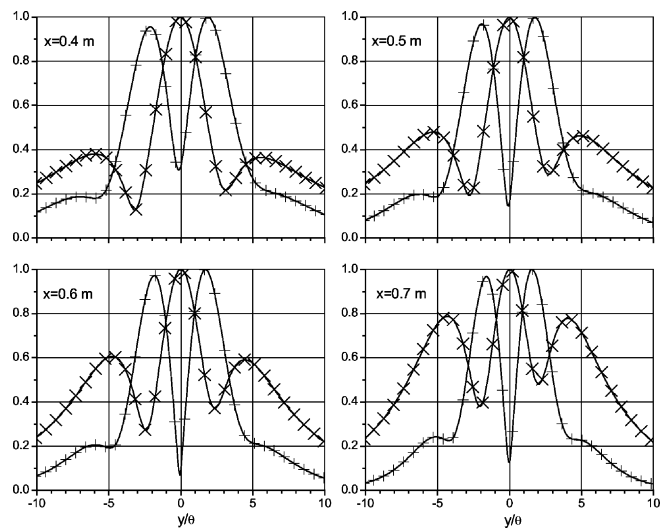

Fig. 6. Profiles of $|u_f|$ (×) and $|u_{2f}|$ (+). $U_1 = 5$ m/s; $U_2 = 3$ m/s. $\varepsilon_0 = 0.1\%$.

In the nonlinear model, the amplitude is found from the Landau-type equation (47). Our numerical results have shown that the nonlinear self-interaction term in (47) is relatively small and the results presented in Fig. 3 remain practically the same, and we conclude that the nonlinear terms are not significant at the amplitudes of interest. Nevertheless, we should emphasize that the main nonlinear effect is associated with the feedback to the mean flow, and it is accounted for in the main order via the mean velocity profile. Only on this background the nonlinear terms in (47) are relatively small.

6. Discussion

The advantage of the triple decomposition method is its adequacy to the experimental procedure where the coherent constituent is extracted from the total signal by means of phase-locked measurements. The governing equations [6] (see Section 2) for the coherent disturbance spell out that the interaction between the coherent and random components might be important and it should be treated somehow. The conventional double decomposition of the total signal into the mean part and the perturbation is, strictly speaking, relevant only to considerations of laminar or transitional flows. The results obtained within the scope of the double decomposition might be interpreted as an analysis of the coherent signal in a turbulent flow only under the assumption that the interaction between the coherent and random fields is negligible. The main (unavoidable) drawback of the triple decomposition method, in turn, is associated with the necessity of choosing a closure hypothesis, and the adequacy of the hypothesis can be checked only by comparison with experimental data.

The successful comparison (Fig. 2) of the theoretical results and the experimental data for the overall amplification leads to the following conclusions:

- interaction between the coherent signal and the random field is important;
- the Newtonian eddy viscosity model for the coherent signal provides the quantitative agreement with the experimental data (the model leads to 'effective' Reynolds number Re_θ about 15);
- the flow divergence must be taken into account to provide a correct comparison of theoretical and experimental data.

These conclusions mean that asymptotic theories at high Reynolds numbers are not relevant to the consideration of organized waves in turbulent mixing layer because they neglect the effect of interaction between the coherent and random disturbances.

Another conclusion that stems from our comparison of theoretical results (Fig. 3) and experimental data [19] is that the approach provides a qualitative explanation of a highly excited mixing layer. It follows from the model that the spreading rate of the mixing layer is governed by the coherent Reynolds stress. At the initial stage, where the coherent Reynolds stress is positive, the spreading rate of the forced mixing layer is higher than in the case of the unforced mixing layer. At some distance downstream, where the coherent signal becomes linearly stable, the Reynolds stress changes its shape and becomes negative. As the amplitude of the coherent signal is high, the Reynolds stress acts as a driving force, suppressing the effect of diffusion due to the eddy viscosity mechanism. The flow is accelerated and the momentum thickness decreases. As the coherent perturbation is damped out farther downstream, the Reynolds stress also becomes smaller and the spreading rate is governed again by the eddy viscosity. As an overall result, the thickness of the mixing layer is smaller than it would be without active control (see Fig. 3). In turn, the comparison of theoretical and experimental data indicates that behind the neutral point, where the coherent Reynolds stresses change its sign, the closure model might be not adequate (the theory overpredicts the length of the zone with a negative spreading rate).

Acknowledgements

The authors are grateful to Professor I. Wygnanski for attracting their interest to the problem of the turbulent mixing layer and for useful discussions of the results. N. Reau thanks the Embassy of France for the support he received during his stay at Tel-Aviv within the framework of the CSN program. This research was supported by a grant from the German–Israeli Foundation for Scientific Research and Development (GIF).

Appendix: Numerical methods

The numerical procedure to treat equation (9) was based on the finite-difference scheme used for the boundary-layer equations [24–26]. We solve (9) separately for the upper ($y > 0$) and lower ($y < 0$) domains. At the boundary $y = 0$, the function $f = 0$, and the velocity $f'(0)$ is iterated to obtain the coincidence of the derivatives $f''(0)$ for the upper and lower domains. At $y \to +\infty$, the boundary condition is $f' \to 1$ and, at $y \to -\infty$, the boundary condition is $f' \to U_2/U_1$.

We used three codes for the stability analysis of the mixing layer:

1. The code based on the two-domain spectral collocation method with Chebyshev polynomials [27] at finite Reynolds number.
2. The code with the fourth-order Runge–Kutta scheme at finite Reynolds number when two pairs of the decaying fundamental solutions are calculated for the upper and lower domains. The general solution is obtained as a sum of the two fundamental solutions for each domain, and an orthonormalization procedure is used during calculation for each pair of fundamental solutions.
3. The code with the fourth Runge–Kutta scheme for the Rayleigh equation.

The code with the spectral collocation method provides a map of eigenvalues for a prescribed frequency and Reynolds number. The eigenvalue problem is reduced to a generalized matrix eigenvalue problem of the form

$$A\mathbf{X} = \alpha B\mathbf{X},$$

where A and B are the square matrices and X is an eigenvector. The problem was solved by means of a standard routine from the NAG or IMSL FORTRAN Libraries. As the Reynolds number is sufficiently high, the code provides an initial eigenvalue for the Rayleigh equation. If the Reynolds number is finite, the code provides an initial eigenvalue for code No. 2.

The analysis of the slow diverging phenomenon was carried out with two codes:

1. The code based on the inviscid equations similar to [9].
2. The code based on the equations with a finite Reynolds number as described in Section 3.

The results from [9] served as the test case for the code No. 2. Afterwards, the second code was tested by comparisons with the first one, when the Reynolds number was chosen to be sufficiently high.

References

[1] H.W. Liepmann, Aspects of the turbulence problem, Z. Angew. Math. Phys. 3 (1952) 407–426.
[2] J. Laufer, New trends in experimental turbulence research, Annu. Rev. Fluid Mech. 7 (1975) 307–326.
[3] A. Roshko, Structure of turbulent shear flows: A new look, AIAA J. 14 (1976) 1349–1357.
[4] B.J. Cantwell, Organized motion in turbulent flow, Annu. Rev. Fluid Mech. 13 (1981) 457–515.
[5] C.M. Ho, P. Huerre, Perturbed free shear layers, Annu. Rev. Fluid Mech. 16 (1984) 365–424.
[6] W.C. Reynolds, A.K.M.F. Hussain, The mechanics of an organized wave in turbulent shear flow. Part 3. Theoretical models and comparisons with experiments, J. Fluid Mech. 54 (1972) 263–288.
[7] A. Michalke, On spatially growing disturbances in an inviscid shear layer, J. Fluid Mech. 23 (1965) 521–544.
[8] P.A. Monkewitz, P. Huerre, Influence of the velocity ratio on the spatial instability of mixing layers, Phys. Fluids 25 (1982) 1137–1143.
[9] M. Gaster, E. Kit, I. Wygnanki, Large scale structures in a forced turbulent mixing layer, J. Fluid Mech. 150 (1989) 23–39.
[10] M. Bouthier, Stabilité linéaire des écoulements presque paralléles par la method des échelles multiples, C. R. Acad. Sci. Sér. A 273 (1971) 1101–1104.
[11] M. Bouthier, Stabilité linéaire des écoulements presque paralléles. Part 1, J. de Mécanique 12 (1973) 75–95.
[12] M. Gaster, On the effects of boundary layer growth on flow stability, J. Fluid Mech. 66 (1974) 465–480.
[13] D.G. Crighton, M. Gaster, Stability of slowly diverging jet flow, J. Fluid Mech. 77 (1976) 397–413.
[14] P. Plaschko, Helical instabilities of slowly divergent jets, J. Fluid Mech. 92 (1979) 209–215.
[15] P. Huerre, M. Rossi, Hydrodynamic instabilities in open flows, in: C. Godreche, P. Manneville (Eds.), Hydrodynamics and Nonlinear Instabilities, Cambridge University Press, Cambridge, 1998, pp. 81–294.
[16] D.R.-S. Ko, T. Kubota, L. Lees, Finite disturbance effect on the stability of laminar incompressible wake behind a flat plate, J. Fluid Mech. 40 (1970) 315–341.
[17] J. Cohen, B. Marasli, V. Levinski, The interaction between the mean flow and coherent structures in turbulent mixing layers, J. Fluid Mech. 260 (1994) 81–94.
[18] D. Oster, I. Wygnanski, The forced mixing layer between parallel streams, J. Fluid Mech. 123 (1982) 91–130.
[19] I. Weisbrot, I. Wygnanski, On coherent structures in highly excited mixing layer, J. Fluid Mech. 195 (1988) 137–159.
[20] P. Huerre, D.G. Crighton, Sound generation by instability waves in a low Mach number jets, AIAA Paper, No. 83-0661, 1983.
[21] P.A. Monkewitz, Subharmonic resonance, pairing and shredding in the mixing layer, J. Fluid Mech. 188 (1988) 232–252.
[22] P. Plaschko, Vortex formation in mixing layers: A weakly nonlinear stability approach, Phys. Fluids 9 (1997) 88–105.
[23] A. Glezer, I. Wygnanski, X. Gu, Amplitude-modulated excitation of turbulent mixing layer, Phys. Fluids A 1 (1989) 1007–1020.
[24] T. Cebeci, P. Bradshow, Momentum Transfer in Boundary Layers, McGraw-Hill, New York, 1977.
[25] T. Cebeci, P. Bradshow, Physical and Computational Aspects of Convective Heat Transfer, Springer, Berlin, 1984.
[26] T. Cebeci, An Engineering Approach to the Calculation of Aerodynamic Flows, Springer, Berlin, 1999.
[27] M.R. Malik, Numerical methods for hypersonic boundary layer stability, J. Comput. Phys. 86 (1990) 376–413.